Biochemical and Biophysical Research Communications 458 (2015) 128–133

Contents lists available at ScienceDirect

Biochemical and Biophysical Research Communications

journal homepage: www.elsevier.com/locate/ybbrc

Characterization of amino acid residues within the N-terminal region of Ubc9 that play a role in Ubc9 nuclear localization

Palak Sekhri [a], Tao Tao [b], Feige Kaplan [c], Xiang-Dong Zhang [a, *]

[a] Department of Biological Sciences, Wayne State University, 5947 Gullen Mall, Detroit, MI 48202, USA
[b] School of Life Sciences, Xiamen University, Xiamen, China
[c] Department of Human Genetics, McGill University, Montreal, Canada

ARTICLE INFO

Article history:
Received 10 January 2015
Available online 27 January 2015

Keywords:
Ubc9
SUMOylation
Importin 13
Nuclear import
Nuclear retention
Nuclear localization

ABSTRACT

As the sole E2 enzyme for SUMOylation, Ubc9 is predominantly nuclear. However, the underlying mechanisms of Ubc9 nuclear localization are still not well understood. Here we show that RNAi-depletion of Imp13, an importin known to mediate Ubc9 nuclear import, reduces both Ubc9 nuclear accumulation and global SUMOylation. Furthermore, Ubc9-R13A or Ubc9-H20D mutation previously shown to interrupt the interaction of Ubc9 with nucleus-enriched SUMOs reduces the nuclear enrichment of Ubc9, suggesting that the interaction of Ubc9 with the nuclear SUMOs may enhance Ubc9 nuclear retention. Moreover, Ubc9-R17E mutation, which is known to disrupt the interaction of Ubc9 with both SUMOs and Imp13, causes a greater decrease in Ubc9 nuclear accumulation than Ubc9-R13A or Ubc9-H20D mutation. Lastly, Ubc9-K74A/S89D mutations that perturb the interaction of Ubc9 with nucleus-enriched SUMOylation-consensus motifs has no effect on Ubc9 nuclear localization. Altogether, our results have elucidated that the amino acid residues within the N-terminal region of Ubc9 play a pivotal role in regulation of Ubc9 nuclear localization.

1. Introduction

Small ubiquitin-related modifiers (SUMOs) are conjugated to many different proteins and thus regulates a variety of cellular processes ranging from cell-cycle progression to gene expression [1,2]. Among three mammalian SUMOs, SUMO-2 and SUMO-3 (SUMO-2/3) are ~95% identical but share only ~45% identity to SUMO-1 [1,2]. SUMOylation is catalyzed by an E1-activating enzyme (SAE1/2), an E2-conjugating enzyme (Ubc9) and multiple E3 ligases [1,2]. Ubc9 receives SUMO from SAE1/2 to form Ubc9~SUMO thioester and then conjugates the SUMO to a lysine (K) residue of a substrate. This K residue is often present within a SUMOylation consensus motif (SCM) (Ψ–K–x–D/E) (Ψ is a hydrophobic residue, x is any residue, and D/E is an acidic residue). Ubc9 can directly bind to SCMs for SUMOylation, which is usually facilitated by an E3 [1,2]. By interacting with SUMOs, SAE1/2, SCMs and E3s, Ubc9 has been considered to play a central role in SUMOylation. Furthermore, both SUMOs and enzymes required for SUMOylation (including SAE1/2 and Ubc9) are predominantly nuclear [3–7], suggesting that SUMOylation mainly occurs in the nucleus. Consistent with this, it has been shown previously that substrates need to be targeted to the nucleus for SUMOylation [7]. Therefore, Ubc9 nuclear localization is expected to be critical for SUMOylation.

The nuclear and cytoplasmic distribution of a protein, such as Ubc9, can be regulated by two major mechanisms [8]. One mechanism is the interaction of this protein with nuclear transport receptors (also called karyopherins) that mediate its nuclear import and export. While the karyopherins mediating nuclear import are called importins, the karyopherins facilitating export are known as exportins. The other mechanism is the interaction of this protein with its nuclear or cytoplasmic anchor proteins, leading to its retention in the nucleus or cytoplasm. Importin 13 (Imp13) has been shown to mediate the nuclear import of Ubc9 using an *in vitro* import assay [9]. However, it is still unclear if Imp13 is exclusively responsible for the primarily nuclear localization of Ubc9.

In this study, we show that RNAi-depletion of Imp13 reduces both Ubc9 nuclear accumulation and global SUMOylation. We further elucidates that Ubc9-R17E mutation, which disrupt its interaction with both Imp13 and SUMOs, causes a greater decrease in the nuclear accumulation of Ubc9 than does Ubc9-R13A

* Corresponding author. Fax: +1 313 5776598.
E-mail address: xzhang@wayne.edu (X.-D. Zhang).

http://dx.doi.org/10.1016/j.bbrc.2015.01.081
0006-291X/

or Ubc9-H20D mutation known to disturb its interaction with SUMOs. Hence, our study reveals the N-terminal amino acid residues of Ubc9 that are critical for Ubc9 nuclear localization.

2. Materials and methods

2.1. Antibodies

Antibodies used in this study include: rabbit anti-Imp13 antibody as previously described [10]; mouse anti-SUMO-1 monoclonal antibody (mAb) (21C7) [11] (Life Technologies); mouse anti-SUMO-2/3 mAb (8A2) [5] (Abcam); rabbit anti-Ubc9 mAb (GeneTex); mouse anti-β-actin mAb (GenScript); mouse anti-α-tubulin mAb (DM1A) (Sigma–Aldrich); rabbit anti-HA antibody (Santa Cruz Biotechnology).

2.2. Cell culture and transfection

Human cervical cancer HeLa cells were cultured in DMEM (Hyclone) supplemented with 10% fetal bovine serum (FBS) (Hyclone) and 1% Penicillin-Streptomycin (Invitrogen). The plasmids and siRNAs were transfected into HeLa cells using Lipofectamine-Plus reagent and Oligofectamine (Invitrogen), respectively. HeLa cells were transfected with non-targeting control siRNAs or each of the three Imp13-specific siRNAs (siRNA 1, 2, and 3) (Dharmacon) (Supplemental Table 1A) for 48 h and the plasmid encoding GFP-tagged Ubc9 for 24 h, and analyzed by immunoblotting and immunofluorescence microscopy.

2.3. Plasmids and site-directed mutagenesis

The open reading frame of human Ubc9 wild-type (WT) was PCR amplified using the primers (Supplemental Table 1B) and subcloned into pEGFP-C1 vector. The pEGFP-C1-Ubc9-WT plasmid was used as a template to generate the constructs encoding GFP-tagged Ubc9-R17E, Ubc9-R13A, Ubc9-H20D, Ubc9-K74A/S89D and Ubc9-R17E/K74A/S89D mutants by site-directed mutagenesis using the PCR primers (Supplemental Table 1C) as previously described [5]. The pcDNA3.1-Imp13-HA construct encoding HA-tagged Imp13-WT as previously described [10] was used as a template to generate the construct encoding Imp13-D426R mutant by site-directed mutagenesis using the PCR primers (Supplemental Table 1D). All the constructs were verified by DNA sequencing.

2.4. Fluorescence microscopy, immunofluorescence microcopy and image analysis

HeLa cells grown on glass coverslip were prepared and analyzed by two approaches. In the first approach, HeLa cells expressing GFP-Ubc9 WT or mutant were fixed with 3.5% paraformaldehyde in PBS for 30 min (without permeabilization) and then analyzed by fluorescence microcopy (Figs. 1B, 3C and 4C). In the second approach, HeLa cells were fixed with 3.5% paraformaldehyde in PBS for 30 min, permeabilized with ice-cold acetone for 5 min, and then analyzed by indirect immunofluorescence microscopy (Fig. 2A). Immunostaining was performed as previously described [12]. Fluorescent images were collected by Olympus inverted IX81 fluorescence microscope with U-Plan S-Apo 60×/1.35 NA oil immersion objective and MicroSuite acquisition software (Olympus). The fluorescence signal intensities of GFP-Ubc9 in the nucleus and cytoplasm were measured using ImageJ software (NIH). 60 cells from each treatment were analyzed to calculate the mean nuclear to cytoplasmic concentration ratio (N/C) of GFP-Ubc9.

3. Results

3.1. RNAi-mediated depletion of Imp13 decreases the nuclear/cytoplasmic concentration ratio of Ubc9 and also levels of SUMOylation

To evaluate the contribution of Imp13-mediated import in Ubc9 nuclear accumulation, we first established a method using RNAi to efficiently knockdown Imp13 expression in HeLa cells (Fig. 1). Our

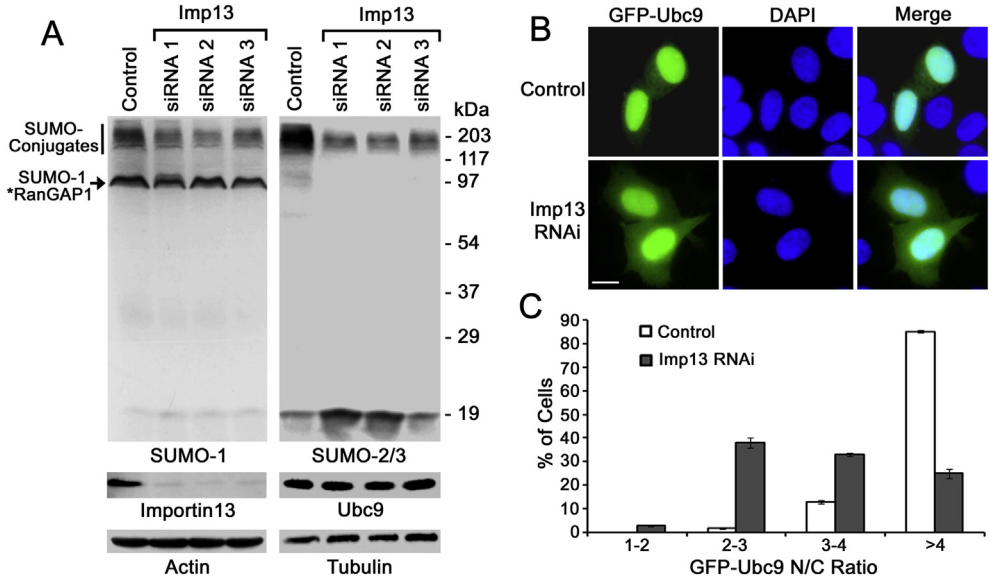

Fig. 1. RNAi-mediated depletion of Imp13 decreases global SUMOylation and the nuclear/cytoplasmic concentration ratio of Ubc9. (A) HeLa cells were transfected with control siRNAs or one of three siRNAs specific to Imp13 (siRNA 1, 2 or 3) and analyzed by immunoblotting. (B) HeLa cells were first transfected with control or Imp13-specific siRNAs for 48 h and then the plasmids encoding GFP-Ubc9 for 24 h. The cells were fixed with paraformaldehyde without permeabilization and then analyzed by fluorescence microscopy. Bar, 10 μm. (C) The histogram shows the percentage of cells exhibiting the mean nuclear/cytoplasmic concentration ratio (N/C) of GFP-Ubc9. The nuclear and cytoplasmic fluorescence intensities of GFP-Ubc9 were quantified using ImageJ (NIH). Each bar represents the mean value ± SEM ($N = 60$, $^*P = 3.5 \times 10^{-18}$, Student's t test).

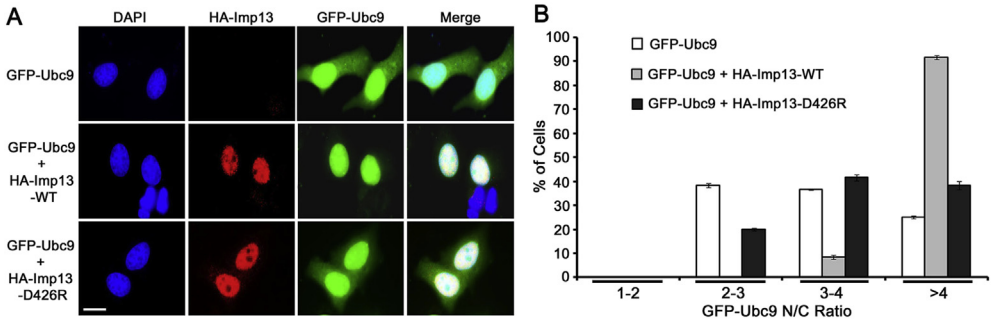

Fig. 2. Imp13-D426R mutation known to interrupt the interaction with Ubc9 *in vitro* nearly abolishes the ability of Imp13 in increasing the nuclear accumulation of Ubc9. (A) HeLa cells were transfected with the plasmids encoding GFP-Ubc9 alone, both GFP-Ubc9 and HA-Imp13-WT, or both GFP-Ubc9 and HA-Imp13-D426R for 48 h, fixed with paraformaldehyde, permeabilized with ice-cold acetone, and then analyzed by indirect immunofluorescence microscopy using anti-HA antibody. Bar, 10 μm. (B) The histogram shows the percentages of cells with the N/C ratios of GFP-Ubc9. Each bar represents the mean value ± SEM ($N = 60$, $^{*}P = 2.8 \times 10^{-16}$ for GFP-Ubc9 vs [GFP-Ubc9 + HA-Imp13-WT], $P = 0.01$ for GFP-Ubc9 vs [GFP-Ubc9 + HA-Imp13-D426R], Student's *t* test).

immunoblot analysis indicated that Imp13 RNAi using three different siRNAs all caused a >90% reduction in Imp13 expression and also a significant decrease in both SUMO-1 and SUMO-2/3 modification (Fig. 1A). Since SUMOylation has been considered to mainly occur in the nucleus, the decreased SUMOylation in Imp13-depleted cells might be caused by a reduced nuclear concentration of Ubc9. To test this, HeLa cells were first transfected with control or Imp13-specific siRNAs for 48 h and then the construct encoding GFP-tagged Ubc9 for 24 h, fixed with 3.5% paraformaldehyde without permeabilization and then analyzed by fluorescence microscopy. We found that compared to control RNAi, Imp13 RNAi caused a decrease in the nuclear/cytoplasmic concentration ratio (N/C) of GFP-Ubc9 (Fig. 1B and C). For example, ~85% of control RNAi cells displayed a high N/C ratio of >4, whereas only ~25% of Imp13 RNAi cells exhibited this high N/C ratio (Fig. 1C). Hence, Imp13-mediated nuclear import is critical for both Ubc9 nuclear accumulation and efficient SUMOylation. However, Ubc9 remains highly enriched in the nucleus in Imp13-depleted cells, suggesting that other mechanism(s) may also regulate Ubc9 nuclear localization.

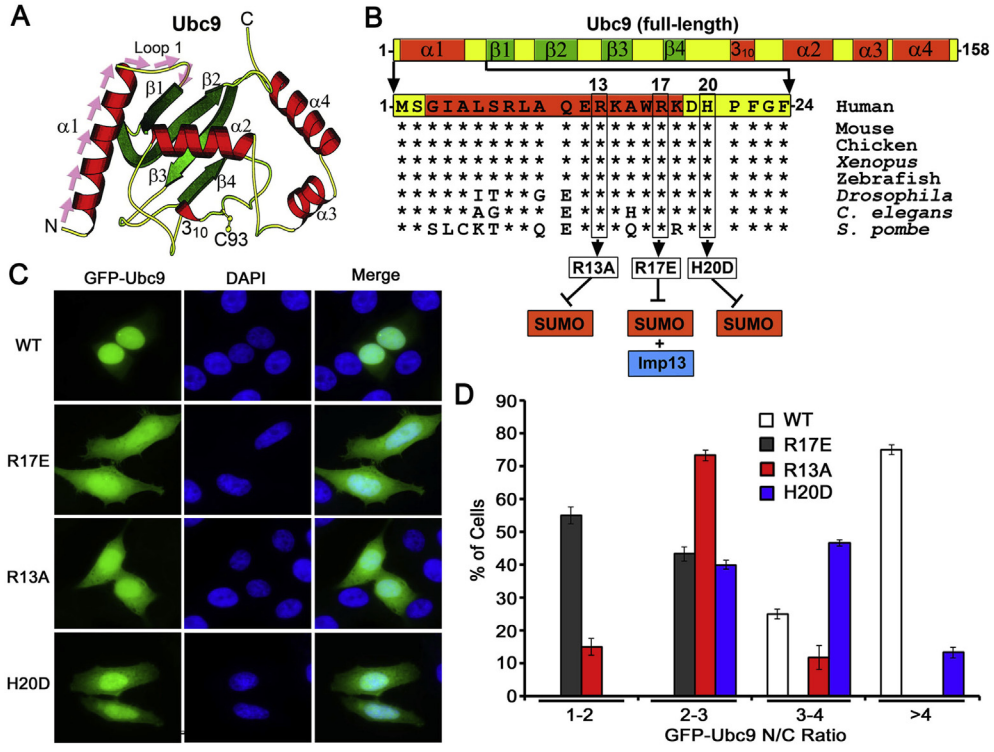

Fig. 3. Ubc9 mutations known to disruption its interaction with nucleus-enriched SUMOs decrease Ubc9 nuclear accumulation. The three Ubc9 single-site mutations include R17E, R13A and H20D. (A) The N-terminal region (1–24 aa) of human Ubc9, including helix α1 and loop 1, is highlighted by pink arrows on the 3D structure of Ubc9 (adapted from Ref. [30]). C93 indicates the catalytic cysteine residue of Ubc9. (B) The three residues R13, R17 and H20 are conserved among various organisms ranging from human to fission yeast (*S. pombe*). While Ubc9-R13A and Ubc9-H20D mutations are known to disrupt its interaction with SUMOs, Ubc9-R17E mutation has been previously shown to interrupt its interactions with both SUMOs and Imp13. (C) HeLa cells were transfected with the constructs encoding GFP-tagged Ubc9-WT, Ubc9-R17E, Ubc9-R13A or Ubc9-H20D for 24 h, fixed with paraformaldehyde without permeabilization and analyzed by fluorescence microscopy. Bar, 10 μm. (D) The histogram shows the percentages of cells with the indicated N/C ratios of GFP-Ubc9. Each bar represents the mean value ± SEM ($N = 60$, $^{*}P = 3.0 \times 10^{-19}$ for Ubc9-WT vs Ubc9-R17E, $^{*}P = 1.0 \times 10^{-15}$ for Ubc9-WT vs Ubc9-R13A, $^{*}P = 1.4 \times 10^{-9}$ for Ubc9-WT vs Ubc9-H20D, Student's *t* test). (For interpretation of the references to color in this figure legend, the reader is referred to the web version of this article.)

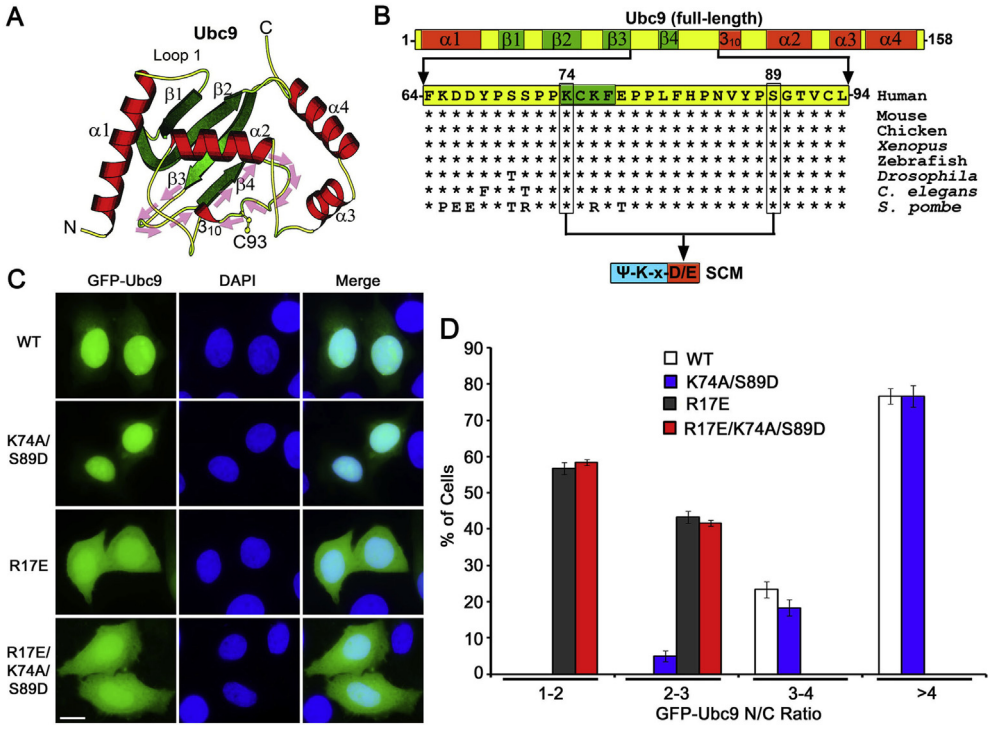

Fig. 4. Ubc9 mutations known to interrupt its interaction with nucleus-enriched SCMs have no effect on Ubc9 nuclear localization. (A) The β4 strand and two flanking loops (64-94 aa) are labeled by pink arrows on the 3D structure of human Ubc9. (B) The K74 and S89 residues within this middle region of Ubc9 (64-94 aa) are highly conserved among various organisms ranging from human to fission yeast (*S. pombe*) and directly interact with the D/E residue within SCMs. (C) HeLa cells were transfected with the constructs encoding GFP-tagged Ubc9-WT, Ubc9-K74A/S89D, Ubc9-R17E or Ubc9-R17E/K74A/S89D mutant for 24 h, fixed with paraformaldehyde without permeabilization and analyzed by fluorescence microscopy. Bar, 10 μm. (D) The histogram indicates the percentages of cells with the indicated N/C ratios of GFP-Ubc9. Each bar represents the mean value ± SEM ($N = 60$, $P = 0.530$ for Ubc9-WT vs Ubc9-K74A/S89D, $P = 0.328$ for Ubc9-R17E vs Ubc9-R17E/K74A/S89D, Student's *t* test). (For interpretation of the references to color in this figure legend, the reader is referred to the web version of this article.)

3.2. Imp13-D426R mutation known to interrupt its interaction with Ubc9 in vitro abolishes the ability of Imp13 in mediating the nuclear accumulation of Ubc9

It has been shown previously that the D426R mutation of Imp13 disrupts its interaction with Ubc9 using *in vitro* binding assays [13]. However, the *in vivo* effect of the Imp13-D426R mutation on Imp13-mediated Ubc9 nuclear import has not been investigated. To address this question, HeLa cells were co-transfected with the constructs encoding GFP-tagged Ubc9 and HA-tagged Imp13-WT or Imp13-D426R mutant. As a negative control, the cells were also transfected with the construct encoding GFP-Ubc9 and the corresponding empty vector. After 48 h of transfection, the cell were fixed with paraformaldehyde, permeabilized with ice-cold acetone, and then analyzed by indirect immunofluorescence microscopy using anti-HA antibody (Fig. 2A). Compared to the control cells, Imp13-WT remarkably increased the percentage of cells with a high N/C ratio of GFP-Ub9 (>4) from ~25% to ~92% (Fig. 2B). However, Imp13-D426R only mildly increased the percentage of cells with this high N/C ratio (>4) from ~25% to ~38%. Hence, the Imp13-D426R mutation inhibits the ability of Imp13 in mediating Ubc9 nuclear import.

3.3. The N-terminal Ubc9 mutations that disrupt its interaction with nucleus-enriched SUMOs reduce the nuclear accumulation of Ubc9

It has been shown previously that Arg17 of Ubc9 (Fig. 3A and B) contacts Asp426, Leu361 and Thr362 of Imp13, and that Ubc9-R17E mutation disrupts in its interaction with Imp13 [13]. Further, GFP-tagged Ubc9-R17E mutant exhibits a striking decrease in its nuclear accumulation compared to GFP-tagged Ubc9-WT [14]. Moreover, we noticed that the nuclear/cytoplasmic ratios of GFP-Ubc9-R17E mutant [14] were much lower than those of GFP-Ubc9-WT in cells with RNAi-depletion of Imp13 (Fig. 1C). One explanation is that Ubc9-R17E mutation not only perturbs its interactions with Imp13 but also with other proteins critical for its nuclear localization. Studies have revealed that Arg17 of Ubc9 contacts Gly81, Glu67 and Asp86 of SUMO-1, and that Ubc9-R17E mutation also abolishes its interaction with nucleus-enriched SUMOs [15,16]. It is thus possible that Ubc9 nuclear localization is also enhanced by its interaction with SUMOs.

To test this, we took the advantage of previous findings that Ubc9-R13A or Ubc9-H20D mutant fails to form complexes with SUMOs [15,16] (Fig. 3B). Structural analyses indicate that Arg13 of Ubc9 interacts with Glu67 of SUMO-1 [15] but does not contact Imp13 [13]. Further, Ubc9-R13A/K13A double mutations have no effect on the 3D structure of Ubc9 [17], suggesting that Ubc9-R13A single mutation is unlikely to alter its structure and thereby its interaction with Imp13. On the other hand, it is still unclear if Ubc9-H20D mutation affects its interaction with Imp13 since the His20 residue of Ubc9 also interacts with Imp13 [16]. HeLa cells were first transfected with the constructs encoding GFP-tagged Ubc9-WT, Ubc9-R17E, Ubc9-R13A and Ubc9-H20D mutants, fixed with paraformaldehyde (without permeabilization), and then analyzed by fluorescence microscopy. Compared to GFP-Ubc9-WT, all of the GFP-Ubc9 mutants displayed a decrease in their N/C ratios (Fig. 4C and D). While ~75% of GFP-Ubc9-WT cells showed a high N/C ratio (>4), none of GFP-Ubc9-R17E or GFP-Ubc9-R13A cells as well as only ~13% of GFP-Ubc9-H20D cells displayed this high ratio (Fig. 4D). On

the other hand, none of GFP-Ubc9-WT cells exhibited a low N/C ratio (1–2: 0%; 2–3: 0%), 100% of R17E cells (1–2: 55%; 2–3: 45%), ~88% of R13A cells (1–2: 15%; 2–3: 73%), and ~40% of H20D cells (1–2: 0%; 2–3: 40%) exhibited this low ratio. Among the three Ubc9 mutants, GFP-Ubc9-R17E exhibited the lowest N/C ratios followed by GFP-Ubc9-R13A and GFP-Ubc9-H20D. Hence, we show that three N-terminal mutations of Ubc9 known to disrupt its interaction with nucleus-enriched SUMOs reduce its nuclear accumulation.

3.4. Ubc9 interaction with nucleus-enriched SCMs does not affect its nuclear localization

Most of SUMOylation (~73%) occur at the lysine residues within the SCMs of primarily nuclear targets [18]. Previous studies indicate that the S89 and K74 residues of Ubc9 are critical for its interaction with SCMs, and that mutations of each residue decreases its binding activity to SCMs [19,20]. To test if the interaction of Ubc9 with nucleus-enriched SCMs enhance its nuclear localization, we generated Ubc9-K74A/S89D double mutant to disrupt the SCM-binding activity of Ubc9 (Fig. 4A and B). HeLa cells were transfected with the constructs encoding GFP-tagged Ubc9-WT or Ubc9-K74A/S89D mutant, fixed with paraformaldehyde (without permeabilization), and analyzed by fluorescence microscopy. We show that Ubc9-K74A/S89D mutant and Ubc9-WT have the similar N/C ratios (Fig. 4C and D), suggesting that Ubc9-K74A/S89D mutations has no effect on its nuclear accumulation. To test whether a defect in Ubc9 interaction with SCMs only exhibits a detectable effect on its nuclear accumulation when this defect is combined with other defects of Ubc9, we generated Ubc9-R17E/K74A/S89D triple mutant with defects in its interaction with SCMs as well as Imp13 and SUMOs. We elucidate that Ubc9-R17E/K74A/S89D share the same N/C ratios with Ubc9-R17E (Fig. 4C and D). Hence, Ubc9 interaction with SCMs is not critical for its nuclear localization.

4. Discussion

In this study, we use RNAi-depletion of Imp13 to show that Imp13-mediated import is critical for Ubc9 nuclear accumulation and efficient SUMOylation. We then reveal that the interaction of Ubc9 with Imp13 and SUMOs but not SCMs are pivotal for Ubc9 nuclear enrichment by analyzing a series of Ubc9 mutations known to disrupt the interaction of Ubc9 with Imp13, SUMOs and/or SCMs. These results support a model that Ubc9 nuclear accumulation is facilitated by Imp13-mediated nuclear import and its interaction with nuclear anchor proteins including SUMOs for nuclear retention. Our study therefore provides a foundation to further investigate how the amino acid residues within the N-terminal region of Ubc9 regulate Ubc9 nuclear localization.

We show that Imp13 RNAi decreases in both N/C ratios of Ubc9 and levels of SUMOylation, suggesting that Ubc9 nuclear accumulation is critical for efficient SUMOylation. Furthermore, we observe that Imp13 RNAi causes a greater reduction in SUMO-2/3 modification than SUMO-1 modification. This result suggests that SUMO-2/3 modification is more sensitive to a reduction in N/C ratios of Ubc9 than SUMO-1 modification. Consistent with this, it has been shown previously that SUMO-2/3 modification is more dynamic than SUMO-1 modification [3].

In this study, we have tested three different commercially available anti-Ubc9 antibodies to evaluate the effect of Imp13 RNAi on the N/C distribution of endogenous Ubc9 using immunofluorescence microscopy. However, these antibodies fail to detect any obvious change in the distribution of Ubc9 in Imp13 RNAi cells compared to control cells although they can recognize endogenous Ubc9 using immunoblot analysis (data not shown). This might be caused by the non-specific staining of these antibodies during immunofluorescence microscopy. Hence, we have evaluated the effect of Imp13 RNAi on the N/C distribution of GFP-tagged Ubc9 instead of endogenous Ubc9. An advantage of using GFP-tagged Ubc9 is that the N/C distribution of GFP-Ubc9 can be well preserved and also conveniently analyzed by fluorescence microscopy after cell fixation without permeabilization. We consistently observe that permeabilization of paraformaldehyde-fixed cells (Fig. 2B) causes a significant reduction in N/C ratios of GFP-Ubc9 compared to the fixed cells without permeabilization (Figs. 1C, 3D and 4D). Consistent with this, it has been shown previously that the nuclear Ubc9 can be extracted by permeabilization of cells [6]. On the other hand, GFP tag (~26 kDa) causes a significant increase in the size of GFP-tagged Ubc9 as Ubc9 has a small size of ~18 kDa. Compared endogenous Ubc9, the larger size of GFP-Ubc9 may decrease its passive diffusion between the nucleus and cytoplasm across NPCs. This might be a reason that we did not observe a highly robust decrease in the N/C ratios of GFP-Ubc9 by RNAi-depletion of Imp13 (Fig. 1C).

We show that Ubc9-R17E mutation, which perturbs the interaction of Ubc9 with both Imp13 and nucleus-enriched SUMOs, causes a greater reduction in the N/C ratios of Ubc9 than RNAi-depletion of Imp13 as well as Ubc9-R13A or Ubc9-H20D mutation known to disrupt in the interaction of Ubc9 with SUMOs. These results suggest that Ubc9 nuclear accumulation is regulated by both Imp13-mediated nuclear import and SUMO-mediated nuclear retention. Further, the R13A, R17E or H20D mutation of Ubc9 does not disturb its 3D structure [15,16], suggesting that the reduction in N/C ratios of these mutants is not caused by a mis-folding of Ubc9. While Ubc9 mutations that interrupt its interaction with the nuclear SUMOs reduces its nuclear enrichment, Ubc9-K74A/S89D mutations that disrupt its interaction with the nucleus-enriched SCMs has no effect on its nuclear accumulation. A possible reason is that Ubc9 has a much higher binding affinity with SUMOs ($K_d = 82 \pm 23$ nM) than with the SCMs of three SUMO substrates ($K_d = 440 \pm 60$ μM for MEF2; $K_d = 457 \pm 87$ μM for HSF1; $K_d = 68 \pm 10$ μM for p53) [16,20].

It has been shown previously that Ubc9-R17E mutation abolishes its interaction with SAE1/2 and the formation of Ubc9~SUMO thioester, Ubc9-R13A mutation reduces both SAE1/2 interaction and thioester formation, and Ubc9-H20D mutation only decreases SAE1/2 interaction without altering thioester formation [15,16,21]. The interaction of Ubc9 with the nucleus-enriched SAE1/2 may also play a role in Ubc9 nuclear accumulation. Hence, it would be worthy to compare the binding affinities of Ubc9-WT and its N-terminal amino acid mutants with Imp13, SUMOs and SAE1/2 in order to better evaluate the contribution of each mutation in Ubc9 nuclear accumulation.

The nuclear import of SAE1/2 is known to be mediated by importin α/β [22]. SAE2 contains a nuclear localization signal (NLS) responsible for its own nuclear import and also the SAE1/2 holoenzyme [22]. Furthermore, SUMOylation of SAE2 at and near its NLS region is required for the nuclear localization of SAE1/2 through nuclear retention [22,23]. SAE1/2 nuclear accumulation is therefore regulated by both importin α/β-mediated nuclear import and SUMOylation-mediated nuclear retention. Similarly, our results support a model that the N-terminal amino acid residues of Ubc9 are critical for Ubc9 nuclear accumulation by facilitating its interactions with Imp13 for nuclear import and also with SUMOs for nuclear retention. Intriguingly, Ubc9 is also modified by SUMO at Lys14 at its N-terminus [24]. Therefore, it would be very interesting to test if SUMOylation of Ubc9 regulates its nuclear localization.

Ubc9 is frequently upregulated in various types of cancers and plays a critical role in cancer progression and metastasis [25–28]. Ubc9 thus represents a novel target for therapeutic treatment of cancers [27,29]. Previous studies and ours reveal that the N-terminal region of Ubc9 regulates not only the formation of

Ubc9~SUMO thioester, an essential step for SUMOylation, but also Ubc9 nuclear localization for efficient SUMOylation by directly interacting with SAE1/2, SUMOs and Imp13 [13–16,21]. It is therefore conceivable that anti-cancer drugs could be developed by targeting this N-terminal region of Ubc9, including helix α1 and loop 1, to disrupt the interaction of Ubc9 with SAE1/2, SUMOs and Imp13, leading to an inhibition of SUMOylation.

Conflict of interest

None declared.

Acknowledgments

We thank Markus Friedrich, Athar Ansari and Jing Zhao for critical comments on the manuscript, all members of the Zhang lab for helpful discussion, Abel Hamdan for assistance on taking fluorescence microscopy images, and Michael Vespremi for support on microscopy. We are grateful to Christopher Lima for valuable advice on generating Ubc9 mutants with a defect in interaction with SUMOylation consensus motif. This work was partially supported by WSU Research Grant 142146 (X.D.Z.) and American Cancer Society Institutional Research Grant 11-053-01-IRG (X.D.Z.).

Transparency document

The transparency document associated with this article can be found in the online version at http://dx.doi.org/10.1016/j.bbrc.2015.01.081.

Appendix A. Supplementary data

Supplementary data related to this article can be found at http://dx.doi.org/10.1016/j.bbrc.2015.01.081.

References

[1] J.R. Gareau, C.D. Lima, The SUMO pathway: emerging mechanisms that shape specificity, conjugation and recognition, Nat. Rev. Mol. Cell. Biol. 11 (2010) 861–871.
[2] Y. Wang, M. Dasso, SUMOylation and deSUMOylation at a glance, J. Cell. Sci. 122 (2009) 4249–4252.
[3] F. Ayaydin, M. Dasso, Distinct in vivo dynamics of vertebrate SUMO paralogues, Mol. Biol. Cell 15 (2004) 5208–5218.
[4] Y. Azuma, S.H. Tan, M.M. Cavenagh, A.M. Ainsztein, H. Saitoh, M. Dasso, Expression and regulation of the mammalian SUMO-1 E1 enzyme, FASEB J. 15 (2001) 1825–1827.
[5] X.D. Zhang, J. Goeres, H. Zhang, T.J. Yen, A.C. Porter, M.J. Matunis, SUMO-2/3 modification and binding regulate the association of CENP-E with kinetochores and progression through mitosis, Mol. Cell 29 (2008) 729–741.
[6] H. Saitoh, M.D. Pizzi, J. Wang, Perturbation of SUMOlation enzyme Ubc9 by distinct domain within nucleoporin RanBP2/Nup358, J. Biol. Chem. 277 (2002) 4755–4763.
[7] M.S. Rodriguez, C. Dargemont, R.T. Hay, SUMO-1 conjugation in vivo requires both a consensus modification motif and nuclear targeting, J. Biol. Chem. 276 (2001) 12654–12659.
[8] M.S. Cyert, Regulation of nuclear localization during signaling, J. Biol. Chem. 276 (2001) 20805–20808.
[9] J.M. Mingot, S. Kostka, R. Kraft, E. Hartmann, D. Gorlich, Importin 13: a novel mediator of nuclear import and export, EMBO J. 20 (2001) 3685–3694.
[10] T. Tao, J. Lan, G.L. Lukacs, R.J. Hache, F. Kaplan, Importin 13 regulates nuclear import of the glucocorticoid receptor in airway epithelial cells, Am. J. Respir. Cell Mol. Biol. 35 (2006) 668–680.
[11] M.J. Matunis, E. Coutavas, G. Blobel, A novel ubiquitin-like modification modulates the partitioning of the Ran-GTPase-activating protein RanGAP1 between the cytosol and the nuclear pore complex, J. Cell. Biol. 135 (1996) 1457–1470.
[12] D. Subramonian, S. Raghunayakula, J.V. Olsen, K.A. Beningo, W. Paschen, X.D. Zhang, Analysis of changes in SUMO-2/3 modification during breast cancer progression and metastasis, J. Proteome Res. 13 (2014) 3905–3918.
[13] M. Grunwald, F. Bono, Structure of Importin13-Ubc9 complex: nuclear import and release of a key regulator of sumoylation, EMBO J. 30 (2011) 427–438.
[14] M. Grunwald, D. Lazzaretti, F. Bono, Structural basis for the nuclear export activity of Importin13, EMBO J. 32 (2013) 899–913.
[15] A.D. Capili, C.D. Lima, Structure and analysis of a complex between SUMO and Ubc9 illustrates features of a conserved E2-Ubl interaction, J. Mol. Biol. 369 (2007) 608–618.
[16] P. Knipscheer, W.J. van Dijk, J.V. Olsen, M. Mann, T.K. Sixma, Noncovalent interaction between Ubc9 and SUMO promotes SUMO chain formation, EMBO J. 26 (2007) 2797–2807.
[17] M.H. Tatham, S. Kim, B. Yu, E. Jaffray, J. Song, J. Zheng, M.S. Rodriguez, R.T. Hay, Y. Chen, Role of an N-terminal site of Ubc9 in SUMO-1, -2, and -3 binding and conjugation, Biochemistry 42 (2003) 9959–9969.
[18] T. Tammsalu, I. Matic, E.G. Jaffray, A.F. Ibrahim, M.H. Tatham, R.T. Hay, Proteome-wide identification of SUMO2 modification sites, Sci. Signal. 7 (2014) rs2.
[19] V. Bernier-Villamor, D.A. Sampson, M.J. Matunis, C.D. Lima, Structural basis for E2-mediated SUMO conjugation revealed by a complex between ubiquitin-conjugating enzyme Ubc9 and RanGAP1, Cell 108 (2002) 345–356.
[20] F. Mohideen, A.D. Capili, P.M. Bilimoria, T. Yamada, A. Bonni, C.D. Lima, A molecular basis for phosphorylation-dependent SUMO conjugation by the E2 UBC9, Nat. Struct. Mol. Biol. 16 (2009) 945–952.
[21] J. Wang, A.M. Taherbhoy, H.W. Hunt, S.N. Seyedin, D.W. Miller, D.J. Miller, D.T. Huang, B.A. Schulman, Crystal structure of UBA2(ufd)-Ubc9: insights into E1-E2 interactions in Sumo pathways, PLoS One 5 (2010) e15805.
[22] M.C. Moutty, V. Sakin, F. Melchior, Importin alpha/beta mediates nuclear import of individual SUMO E1 subunits and of the holo-enzyme, Mol. Biol. Cell 22 (2011) 652–660.
[23] K. Truong, T.D. Lee, B. Li, Y. Chen, Sumoylation of SAE2 C terminus regulates SAE nuclear localization, J. Biol. Chem. 287 (2012) 42611–42619.
[24] P. Knipscheer, A. Flotho, H. Klug, J.V. Olsen, W.J. van Dijk, A. Fish, E.S. Johnson, M. Mann, T.K. Sixma, A. Pichler, Ubc9 sumoylation regulates SUMO target discrimination, Mol. Cell 31 (2008) 371–382.
[25] Y.Y. Mo, Y. Yu, E. Theodosiou, P.L. Ee, W.T. Beck, A role for Ubc9 in tumorigenesis, Oncogene 24 (2005) 2677–2683.
[26] H. Li, H. Niu, Y. Peng, J. Wang, P. He, Ubc9 promotes invasion and metastasis of lung cancer cells, Oncol. Rep. 29 (2013) 1588–1594.
[27] Y.Y. Mo, S.J. Moschos, Targeting Ubc9 for cancer therapy, Expert Opin. Ther. Targets 9 (2005) 1203–1216.
[28] S.J. Moschos, A.P. Smith, M. Mandic, C. Athanassiou, K. Watson-Hurst, D.M. Jukic, H.D. Edington, J.M. Kirkwood, D. Becker, SAGE and antibody array analysis of melanoma-infiltrated lymph nodes: identification of Ubc9 as an important molecule in advanced-stage melanomas, Oncogene 26 (2007) 4216–4225.
[29] M. Hirohama, A. Kumar, I. Fukuda, S. Matsuoka, Y. Igarashi, H. Saitoh, M. Takagi, K. Shin-ya, K. Honda, Y. Kondoh, T. Saito, Y. Nakao, H. Osada, K.Y. Zhang, M. Yoshida, A. Ito, Spectomycin B1 as a novel SUMOylation inhibitor that directly binds to SUMO E2, ACS Chem. Biol. 8 (2013) 2635–2642.
[30] H. Tong, G. Hateboer, A. Perrakis, R. Bernards, T.K. Sixma, Crystal structure of murine/human Ubc9 provides insight into the variability of the ubiquitin-conjugating system, J. Biol. Chem. 272 (1997) 21381–21387.